Chitosan Electrospun Nanofibers Web

AKBAR K. HAGHI*, MOHAMMAD KANAFCHIAN , MOTAHAREH KANAFCHIAN
University of Guilan, Rasht, Iran

The chitosan based nanofibers web is a biocompatible, biodegradable, antimicrobial and non-toxic structure which has both physical and chemical properties to effectively capture and neutralize toxic pollutants from air and liquid media. Despite such potentials, the mechanical properties of nanofibers web is very poor to use in filtration applications. To remedy this defect, nanofibers web could laminate into a strength structure. The purpose of this study is to consider the influence of laminating temperature on nanofibers web/multilayer structure properties. The nanofibers web morphology and multilayer cross-section was observed under an optical microscope and scanning electron microscope, respectively. Also, air permeability experiments were performed to examine the effect of laminating temperature on air transport properties of multilayer structures. Optical microscope images showed that the nanofiber web began to damage when laminating temperature was selected above melting point of adhesive layer. Air permeability decreased with increasing laminating temperature. It is also observed that the adhesive force between layers was increased by increasing laminating temperature.

Keywords: chitosan, nanofibers web, filtration, lamination

There is an enormous requirement for cleaner air around the world which has activated immense interest in the development of high efficiency filters or face masks. Nonwoven nanofibrous media have low basis weight, high permeability, and small pore size that make them appropriate for a wide range of filtration applications. In addition, nanofibers web offers unique properties like high specific surface area (ranging from 1 to 35m^2/g depending on the diameter of fibers), good interconnectivity of pores and the potential to incorporate active chemistry or functionality on nanoscale. To date, the most successful method of producing nanofibers is through the process of electrospinning. The electrospinning process uses high voltage to create an electric field between a droplet of polymer solution at the tip of a needle and a collector plate. When the electrostatic force overcomes the surface tension of the drop, a charged, continuous jet of polymer solution is ejected. As the solution moves away from the needle and toward the collector, the solvent evaporates and jet rapidly thins and dries. On the surface of the collector, a nonwoven web of randomly oriented solid nanofibers is deposited [1]. It has been found that the morphology of the web, such as fiber diameter and its uniformity of the electrospun nanofibers, are dependent on many processing parameters. These parameters can be divided into three main groups: A) solution properties, B) processing conditions, C) ambient conditions. Each of the parameters has been found to affect the morphology of the electrospun fibers.

Solution Properties

Parameters such as viscosity of solution, solution concentration, molecular weight of polymer, electrical conductivity, elasticity and surface tension have an important effect on the morphology of nanofibers.

Viscosity

The viscosity range of a different nanofiber solution which is spinnable is different. One of the most significant parameters influencing the fiber diameter is the solution viscosity. A higher viscosity results in a large fiber diameter. Beads and beaded fibers are less likely to be formed for the more viscous solutions. The bead diameter becomes bigger and the average distance between beads on the fibers become longer as the viscosity increases.

Solution concentration

In the electrospinning process, for fiber formation to occur a minimum solution concentration is required. As the solution concentration increases, a mixture of beads and fibers is obtained. The shape of the beads changes from spherical to spindle-like when the solution concentration varies from low to high levels. The fiber diameter increases with increasing solution concentration because of the higher viscosity resistance. Nevertheless, at higher concentration the viscoelastic force which usually resists rapid changes in fiber shape may result in uniform fiber formation. However, it is impossible to electrospinning if the solution concentration or the corresponding viscosity become too high due to the difficulty in liquid jet formation.

Molecular weight

Molecular weight also has a significant effect on the rheological and electrical properties such as viscosity, surface tension, conductivity and dielectric strength. It has been observed that too low molecular weight solution tends to form beads rather than fibers and high molecular weight nanofiber solution gives fibers with larger average diameter.

Surface tension

The surface tension of a liquid is often defined as the force acting at right angles to any line of unit length on the liquid surface. By reducing surface tension of a nanofiber solution, fibers could be obtained without beads. The surface tension seems more likely to be a function of solvent compositions, but is negligibly dependent on the solution concentration. Different solvents may contribute to different surface tensions. However, a lower surface tension of a solvent will not necessarily always be more

* email: Haghi@Guilan.ac.ir

suitable for electrospinning. Generally, surface tension determines the upper and lower boundaries of electrospinning window if all other variables are held constant. The formation of droplets, bead and fibers can be driven by the surface tension of solution, and lower surface tension of the spinning solution helps electrospinning to occur at lower electric field.

Solution Conductivity

There is a significant drop in the diameter of the electrospun nanofibers when the electrical conductivity of the solution increases. Beads may also be observed due to low conductivity of the solution, which results in insufficient elongation of a jet by electrical force to produce uniform fiber. In general, electrospun nanofibers with the smallest fiber diameter can be obtained with the highest electrical conductivity. This indicates that the drop in the size of the fibers is due to the increased electrical conductivity.

Processing conditions

Another important parameter that affects the electrospinning process is the various external factors exerting on the electrospinning jet. This includes the applied voltage, the feed rate, diameter of nuzzle/needle and distance between the needle and collector.

Applied Voltage

In the case of electrospinning, the electric current due to the ionic conduction of charge in the nanofiber solution is usually assumed small enough to be negligible. The only mechanism of charge transport is the flow of solution from the tip to the target. Thus, an increase in the electrospinning current generally reflects an increase in the mass flow rate from the capillary tip to the grounded target when all other variables (conductivity, dielectric constant, and flow rate of solution to the capillary tip) are held constant. Increasing the applied voltage (*i.e.*, increasing the electric field strength) will increase the electrostatic repulsive force on the fluid jet, which favors the thinner fiber formation. On the other hand, the solution will be removed from the capillary tip more quickly as jet is ejected from Taylor cone. This results in the increase of the fiber diameter.

Feed Rate

The morphological structure can be slightly changed by changing the solution flow rate. When the flow rate exceeded a critical value, the delivery rate of the solution jet to the capillary tip exceeded the rate at which the solution was removed from the tip by the electric forces. This shift in the mass-balance resulted in sustained but unstable jet and fibers with big beads formation. In the first part of this study, the production of electrospun nanofibers was investigated. In another part, a different case study was presented to show how nanofibers can be laminated for application in filter media.

Distance between the needle and collector

When the distance between the tip of needle and the collector is reduced, the jet will have a shorter distance to travel before it reaches the collector plate. Moreover, the electric field strength will also increase at the same time and this will increase the acceleration of the jet to the collector. As a result, there may not have enough time for the solvents to evaporate when it hits the collector.

Diameter of Needle

The internal diameter of needle has a certain effect on the electrospinning process. A smaller internal diameter was found to reduce the amount of beads on the electrospun web and was also found to cause a reduction in the diameter of fibers.

Ambient conditions

Since electrospinning is influenced by external electric field, any changes in the electrospinning environment will also affect the electrospinning process. Any interaction between the surrounding and the polymer solution may have an effect on the electrospun fiber morphology. For example, high humidity was found to cause the formation of pores on the surface of the fibers [2,4].

Chitosan

Over the recent years, interest in the application of naturally occurring polymers such as polysaccharides and proteins, owing to their abundance in the environment, has grown considerably. Chitin, the second most abundant polysaccharide found on earth next to cellulose, is a major component of the shells of crustaceans such as crab, shrimp and crawfish. The structural characteristics of chitin are similar to those of glycosaminoglycans. When chitin is deacetylated over about 60% it becomes soluble in dilute acidic solutions and is referred to chitosan or poly(N-acetyl-D-glucosamine). Chitosan and its derivatives have attracted much research because of their unique biological properties such as antibacterial activity, low toxicity, and bio-degradability [5, 7].

Depending on the chitin source and the methods of hydrolysis, chitosan varies greatly in its molecular weight (MW) and degree of deacetylation (DDA). The MW of chitosan can vary from 30 kDa to well above 1000 kDa and its typical DDA is over 70 %, making it soluble in acidic aqueous solutions. At a *p*H of about 6–7, the biopolymer is a polycation and at a *p*H of 4.5 and below, it is completely protonated. The fraction of repeat units which are positively charged is a function of the degree of deacetylation and solution *p*H. A higher degree of deacetylation would lead to a larger number of positively charged groups on the chitosan backbone [8]. Also, Sorlier et al. [9] have studied the effect of *p*H and DDA on Chitosan solution pKa and found that for varying DDA from 5 to 75%, pKa varies between 6.3 and 7.2.

As mentioned above, chitosan has several unique properties such as the ability to chelate ions from solution and to inhibit the growth of a wide variety of fungi, yeasts and bacteria. Although the exact mechanism with which chitosan exerts these properties is currently unknown, it has been suggested that the polycationic nature of this piopolymer that forms from acidic solutions below *p*H 6.5 is a crucial factor. Thus, it has been proposed that the positively charged amino groups of the glucosamine units interact with negatively charged components in microbial cell membranes altering their barrier properties, thereby preventing the entry of nutrients or causing the leakage of intracellular contents. Another reported mechanism involves the penetration of low MW chitosan in the cell, the binding to DNA, and the subsequent inhibition of RNA and protein synthesis. Chitosan has been shown also to activate several defense processes in plant tissues, and it inhibits the production of toxins and microbial growth because of its ability to chelate metal ions [10, 12].

Electrospinning of Chitosan

Chitosan is insoluble in water, alkali, and most mineral acidic systems. However, though its solubility in inorganic acids is quite limited, chitosan is in fact soluble in organic acids, such as dilute aqueous acetic, formic, and lactic

acids. Chitosan also has free amino groups, which makes it a positively charged polyelectrolyte. This property makes chitosan solutions highly viscous and complicates its electrospinning [13].Furthermore, the formation of strong hydrogen bonds in a 3-D network prevents the movement of polymeric chains exposed to the electrical field [14]. Different strategies were used for bringing chitosan in nanofiber form. The three top most abundant techniques include blending of favorite polymers for electrospinning process with chitosan matrix [15, 16] alkali treatment of chitosan backbone to improve electro spinnability through reducing viscosit y [17] and employment of concentrated organic acid solution to produce nanofibers by decreasing of surface tension [18]. Electrospinning of polyethylene oxide(PEO)/chitosan [15] and polyvinyl alcohol(PVA)/ chitosan [16] blended nanofiber are two recent studies based on first strategy. In the second protocol, the MW of chitosan decreases through alkali treatment. Solutions of the treated chitosan in aqueous 70-90% acetic acid produce nanofibers with appropriate quality and processing stability [17]. Using concentrated organic acids such as acetic acid [18] and triflouroacetic acid (TFA) with and without dichloro-methane (DCM) [19] has been reported exclusively for producing neat chitosan nanofibers. They similarly reported the decreasing of surface tension and at the same time enhancement of charge density of chitosan solution without significant effect on viscosity. This new method suggests significant influence of the concentrated acid solution on the reducing of the applied field required for electrospinning.

The mechanical properties of neat chitosan electrospun natural nanofibers web can be improved by addition of the synthetic materials including carbon nanotubes (CNTs) [20]. CNTs are one of the important synthetic materials that were discovered by Iijima in 1991 [21]. CNTs, either single-walled nanotubes (SWNTs) or multiwalled nanotubes (MWNTs), combine the physical properties of diamond and graphite. They are extremely thermally conductive like diamond and appreciably electrically conductive like graphite. Moreover, the flexibility and exceptional specific surface area to mass ratio can be considered as significant properties of CNTs. Scientists are becoming more interested in CNTs for existence of exclusive properties such as mechanical strength for various applications [22].

Laminating of Electrospun web

While electrospun webs suggest exciting characteristics, it has been reported that they have limited mechanical properties [23, 24]. To compensate this drawback in order to use them in filtration applications, electrospun nanofibers web could be laminated via an adhesive into a multilayer system [25-28].The adhesives are as solvent/water-based adhesive or as hot-melt adhesive. At the first group, the adhesives are as solution in solvent or water, and solidify by evaporating of the carrying liquid. Solvent-based adhesives could 'wet' the surfaces to be joined better than water-based adhesives, and also could solidify faster. But unfortunately, they are environmentally unfriendly, usually flammable and more expensive than those. Of course it does not mean that the water-based adhesives are always preferred for laminating, since in practice, drying off water in terms of energy and time is expensive too. Besides, water-based adhesives are not resisting to water or moisture because of their hydrophilic nature. At the second group, hot-melt adhesives are environmentally friendly, inexpensive, require less heat and energy, and so are now more preferred. Generally there are two procedures to melt these adhesives; static hot-melt laminating that accomplish by flat iron or Hoffman press and continuous hot-melt laminating that uses the hot calendars. In addition, these adhesives are available in several forms; as a web, as a continuous film, or in powder form. The adhesives in film or web form are more expensive than the corresponding adhesive powders. The web form are discontinuous and produce laminates which are flexible, porous and breathable, whereas, continuous film adhesives cause stiffening and produce laminates which are not porous and permeable to both air and water vapour. This behaviour is attributed to impervious nature of adhesive film and its shrinkage under the action of heat [29]. Thus, the knowledge of laminating skills and adhesive types is very essential to producing appropriate multilayer structures. Specifically, this subject becomes more highlight as we will laminate the ultrathin nanofibers web, because the laminating process may be adversely influenced on the nanofibers web properties. Lee et al. [30] without disclosure of laminating details, reported that the hot-melt method is more suitable for nanofiber web laminating. In this method, laminating temperature is one of the most effective parameters. Incorrect selection of this parameter may lead to change or damage ultrathin nanofiber web. Therefore, it is necessary to find out a laminating temperature which has the least effect on nanofiber web during process.

The purpose of this study is to consider the influence of laminating temperature on the nanofibers web/multilayer structure properties. Multilayer structures were made by laminating of nanofibers web into cotton fabric via hot-melt method at different temperatures. Effects of laminating temperature on the nanofibers web morphology, air transport properties and the adhesive force were discussed.

Experimental part

Preparation of chitosan-MWNT solution

Chitosan with DDA of 85% and MW of 5×10^5 was supplied by Sigma-Aldrich. The MWNTs, supplied by Nutrino, have an average diameter of 4 nm and purity of about 98%. All of the other solvents and chemicals were commercially available and used as received without further purification. A Branson Sonifier 250 operated at 30W used to prepare the MWNT dispersion in chitosan/organic acid solution (70/ 30 TFA/DCM). First, 3mg of as received MWNTs was dispersed into deionized water or DCM using solution sonicating for 10min. Next, chitosan was added to MWNTs dispersion to prepare a 10 wt% solution after sonicating for 5min. Finally, in order to obtain a chitosan/MWNT solution, organic acid solution was added and the dispersion was stirred for 10 h.

Electrospinning

After the preparation of spinning solution, it was inserted into a syringe with a stainless steel nozzle and then the syringe was placed in a metering pump from WORLD PRECISION INSTRUMENTS (Florida, USA). Next, this set installed on a homemade plate which it could traverse to left-right direction along drum collector (fig.1). The electrospinning conditions and layers properties for laminating are summarized in table 1. The electrospinning process was carried out for 8h and the electrospun fibres were collected on an aluminium-covered rotating drum which was previously covered with a Poly-Propylene Spun-bond Nonwoven (PPSN) substrate. After removing of PPSN covered with electrospun fibres from drum and attaching another layer of PPSN on it, this set was incorporated

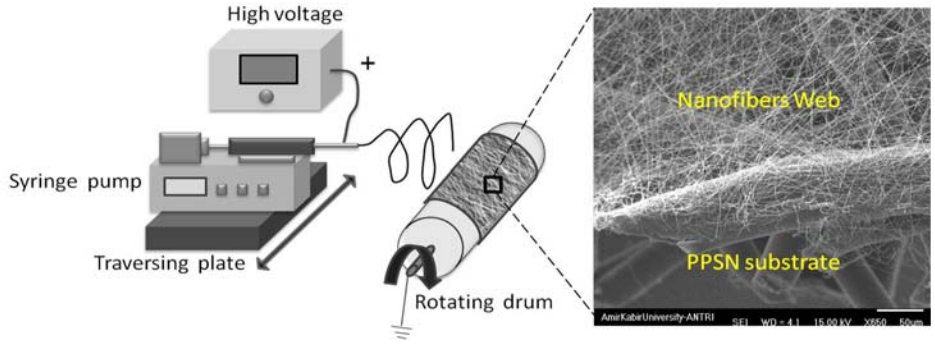

Fig.1. Electrospinning setup and an enlarged image of Nanofibers Web on PPSN

Electrospinning conditions		Layers properties	
		PPSN	
Polymer concentration	12% w/w		Thickness
0.19 mm			
Feed rate	1 µl/h		Air permeability
824 cm³/s/cm²			
		Melting	point
140°C			
Nozzle inner diameter	0.4 mm	Mass	25
g/m²			
Nozzle-Drum distance	7 cm	Electrospun web	
Voltage	11 KV	Mass	3.82
g/m²			
Traversing plate speed	0.4 m/min	Fabric	
Drum speed	9 m/min		Thickness
0.24 mm			
Spinning Time	8 hr		Warp-weft density
25×25 per cm			

Table1
ELECTROSPINNING CONDITIONS AND LAYERS PROPERTIES FOR LAMINATING

between two cotton weft-warp fabrics as a structure of fabric-PPSN-nanofibers web-PPSN-fabric (fig. 2). Finally, hot-melt laminating performed using a simple flat iron for 1min, under a pressure of 9gf/cm^2 and at temperatures 85,110,120,140,150°C (above softening point of PPSN) to form multilayer structures.

Characterizations

The morphology of Electrospun fibers

The electrospun fibers were characterized using scanning electron microscope (SEM, Seron Technology, AIS-2100, Korea) to study the fiber morphology. The sample was sputter coated with Au/Pd to prevent charging during SEM imaging. Image processing software (MICRO-STRUCTURE MEASUREMENT) was used to measure the fiber diameter from the SEM micrograph. Fiber diameter was measured at 50 different points for determining the average and distribution of diameter. The mass per unit area (g/m^2 or gsm) of the electrospun web was measured by dividing the mass of the web by its area.

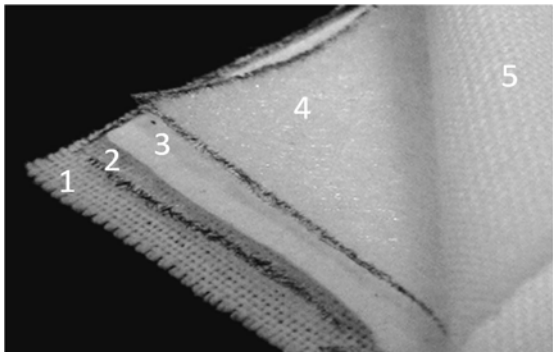

Fig. 2. Multilayer components: (1) Fabric, (2) PPSN, (3) Nanofibers Web, (4) PPSN, (5) Fabric

The morphology of Multilayer structures

A piece of each multilayer was frozen fractured in liquid nitrogen and after sputter-coating with Au/Pd, a cross-section image of them captured using a scanning electron microscope.

Also, to consider the nanofiber web surface after hot-melt laminating, other laminations were prepared by a non-stick sheet made of Teflon (0.25 mm thickness) as a replacement for one of the fabrics (fabric/PPSN/nanofibers web/PPSN/Teflon sheet). Laminating process was carried out at the same conditions which mentioned to produce primary laminations. Finally, after removing of Teflon sheet, the nanofibers layer side was observed under an optical microscope (MICROPHOT-FXA, Nikon, Japan) connected to a digital camera.

Measurement of Air permeability

The air permeability of multilayer structures, which is a measure of the structural porosity, was measured by air permeability tester (TEXTEST FX3300, Zürich, Switzerland). There were tested 5 pieces of each sample under air pressure of 125 Pa, at ambient condition (16°C, 70%RH), and then the average air permeability was calculated.

Results and discussions

In our previous work, chitosan/MWNTs nanofibers web was fabricated using electrospinning technique, successfully [31]. The goal of this research is to develop chitosan based multilayer structures in order to use them in filtration applications. In electrospinning phase, PPSN was chosen as a substrate to provide strength to the nanofiber web and to prevent its destruction in removing from the collector. In figure 1, an ultrathin layer of nanofibers web on PPSN layer is illustrated, which conveniently shows the relative fiber size of nanofiber (326±68 nm) web compared to PPSN fibers. Also, this Figure shows that the

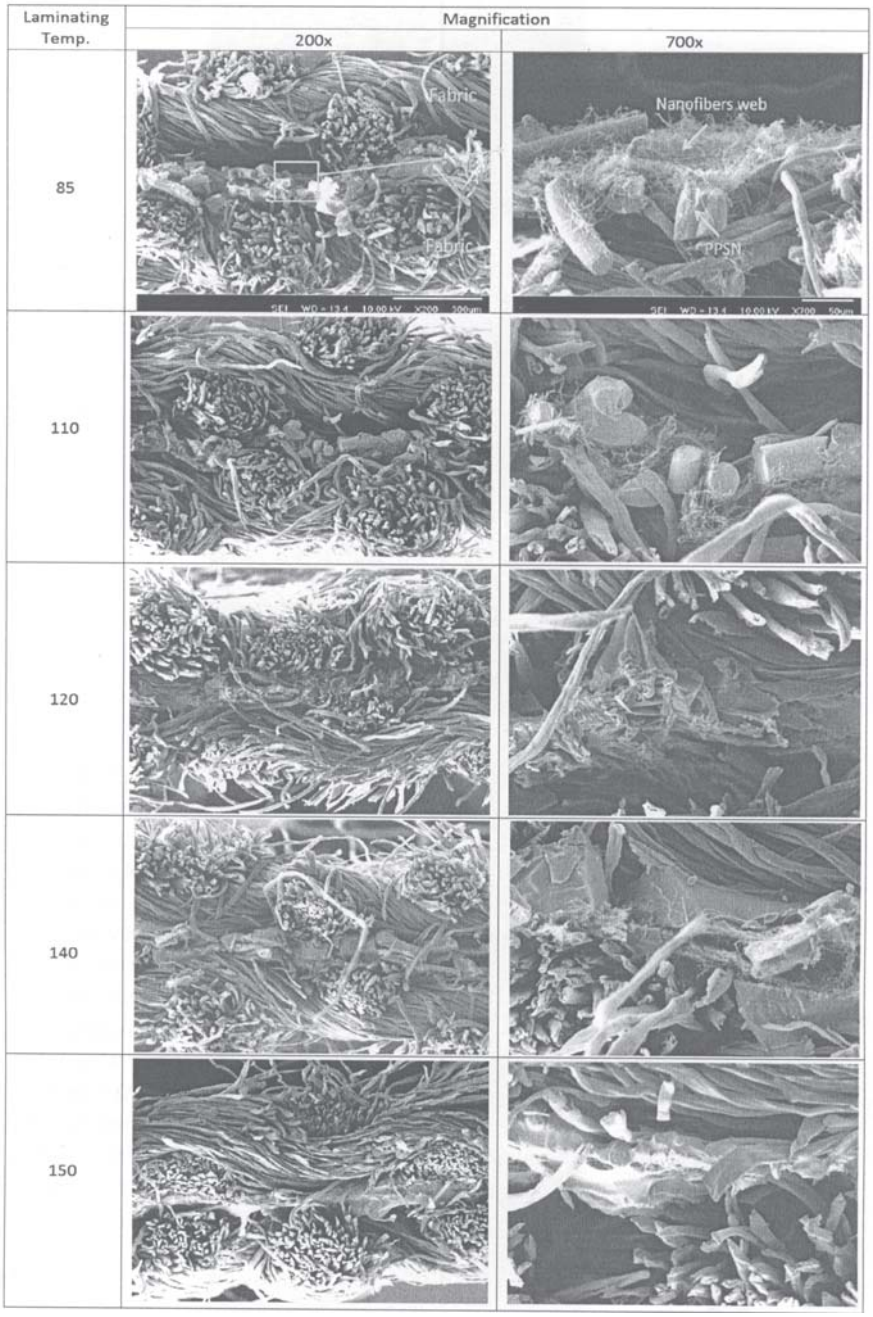

Fig. 3. SEM images of multilayer fabric cross-section at different laminating temperatures

macropores of PPSN substrate is covered with numerous electrospun nanofibers, which will create innumerable microscopic pores in this system. But in laminating phase, this substrate acts as an adhesive and causes to bond the nanofiber web to the fabric. In general, it is relatively simple to create a strong bond between these layers, which guarantees no delamination or failure in multilayer structures; the challenge is to preserve the original properties of the nanofiber web and fabrics. In other words, the application of adhesive should have minimum effect on the fabric or nanofiber web structure. In order to achieve this aim, it is necessary that: a) the least amount of a highly effective adhesive applied, b) the adhesive correctly cover the widest possible surface area of layers for better linkage between them and c) the adhesive penetrate to a certain extent of the nanofiber web/fabric [29]. Therefore, we selected PPSN, which is a hot-melt adhesive in web form. As mentioned above, the perfect use of web form adhesive can be lead to produce multilayer fabrics which are porous, flexible and permeable to both air and water vapour. On the other hand, since the melting point of PPSN is low, hot-melt laminating can perform at lower temperatures. Hence, the probability of shrinkage that may happen on layers in effect of heat becomes smaller. Of course, the thermal degradation of chitosan nanofiber web begins above 250°C [32, 33] and the cotton fabrics are intrinsically resistant to heat too. By this description, laminating process was performed at five different temperatures to consider the effect of laminating temperature on the nanofiber web/multilayer properties.

The SEM images of multilayer fabric cross-section after laminating at different temperatures are shown in figure 3. It is obvious that these images cannot deliver useful information about nanofibers web morphology in multilayer structure, so it becomes impossible to consider the effect of laminating temperature on nanofibers web. Hence, in a novel way, we decided to prepare a secondary multilayer by substitution of one of the fabrics with Teflon sheet. By this replacement, the surface of nanofiber web will become accessible after laminating because Teflon is a non-stick material and easily separates from the adhesive.

Figure 4 presents optical microscope images of nanofiber web and adhesive after laminating at different temperatures. It is apparent that the adhesive gradually flattened on nanofiber web (fig. 4(a-c)) when laminating

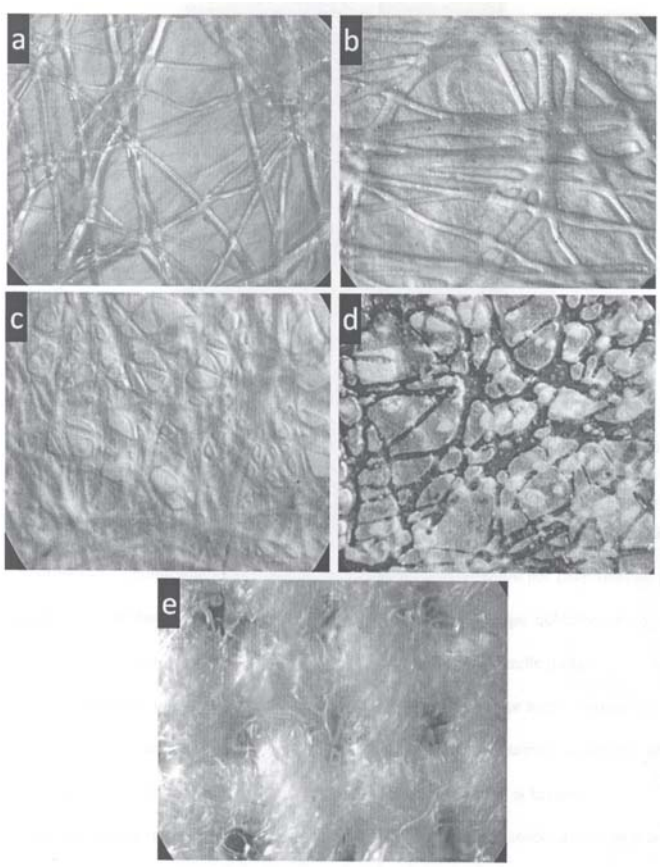

Fig.4. The optical microscope images of nanofiber web surface at different laminating temperatures (100x magnification), a) 85°C, b) 110°°C, c) 120°C, d) 140°C and e) 150°C.

temperature increased to melting point of adhesive (140 °C). This behaviour is attributed to increment in plasticity of adhesive because of temperature rise and the pressure applied from the iron weight. But, by selection of melting point as laminating temperature, the adhesive completely melted and began to penetrate into the nanofiber web structure instead of spread on it (fig. 4(d)). This penetration, in some regions, was continued to some extent so the adhesive was even passed across the web layer. The dark crisscross lines in figure 4(d) obviously show wherever this excessive penetration is occurred. The adhesive penetration could intensify by increasing the laminating temperature above melting point; because the fluidity of melted adhesive increases by temperature rise. Figure 4(e) clearly shows the amount of adhesive diffusion in the web which was laminated at 150°C. At this case, the whole diffusion of adhesive lead to create a transparent film and to appear the fabric structure under optical microscope.

Also, to examine how laminating temperature affect the permeability of multilayer structure, air permeability experiment was performed. The bar chart in figure 5 indicates the effect of laminating temperature on air transport properties of multilayer. As might be expected, the air permeability decreased with increasing laminating temperature. This procedure means that the air permeability of multilayer fabric is related to adhesive's form after laminating because at these temperatures the nanofiber web and cotton fabrics intrinsically are resistant to heat. Of course, it is to be noted that the pressure applied during laminating can leads to compact the web/fabric structure and to reduce the air permeability too. Nevertheless, this parameter did not have effective role on air permeability variations at this work, because the pressure applied for all samples had the same quantity. As

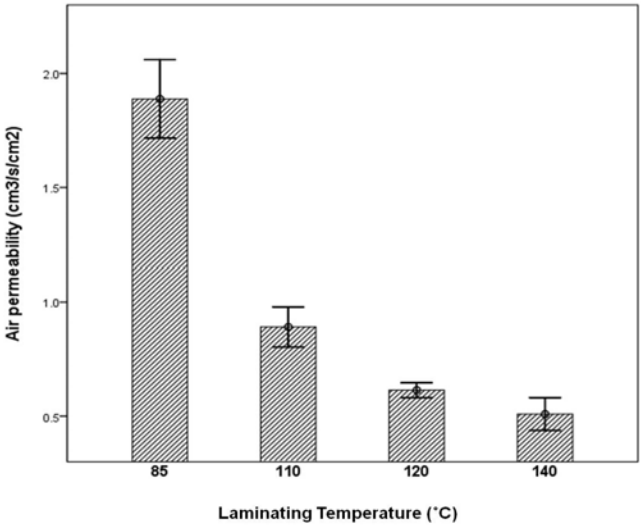

Fig. 5. Air permeability of multilayer structure after laminating at different temperatures

discussed, by increasing of laminating temperature to melting point, PPSN was gradually flattened between layers so that it was transformed from web-form to film-like. It is obvious in figure 4(a-c) that the pore size of adhesive layer becomes smaller in effect of this transformation. Therefore, we can conclude that the adhesive layer, as a barrier, resists to convective air flow during experiment and finally reduces the air permeability of multilayer fabric according to the pore size decrease. But, this conclusion is unacceptable for the samples laminated at melting point (140°C) since the adhesive was missed self layer form in effect of penetration into the web/fabric structures (fig. 4d). At these samples, the adhesive penetration leads to block the pores of web/fabrics and to prevent of the air pass during experiment. It should be noted that the adhesive was penetrated into the web much more than the fabric because, PPSN structurally had more surface junction with the web (fig. 3). Therefore here, the nanofiber web absorbs the adhesive and forms an impervious barrier to air flow.

Furthermore, we only observed that the adhesive force between layers was improved according to temperature rise. For example, the samples laminated at 85°C exhibited very poor adhesion between the nanofiber web and the fabrics as much as they could be delaminated by light abrasion of thumb, as illustrated at figure 3. Generally, it is essential that no delamination occurs during use of this multilayer structure, because the nanofiber web might be destroyed due to abrasion of other layers. Before melting point, improving the adhesive force according to temperature rise is simultaneously attributed to the more penetration of adhesive into layers and the expansion of bonding area between them, as already discussed. Also at melting point, the deep penetration of adhesive into the web/fabric leads to increase in this force.

Conclusions

In this study, the effect of laminating temperature on the nanofibers web/multilayer structures properties investigated to make next generation of filter media. First, we demonstrate that it is impossible to consider the effect of laminating temperature on the nanofiber web morphology by a SEM image of multilayer cross-section. Thus, we prepared a surface image of nanofiber web after laminating at different temperature using an optical microscope. It was observed that nanofiber web was

approximately unchanged when laminating temperature was below PPSN melting point. In addition, to compare air transport properties of multilayer fabrics, air permeability tests were performed. It was found that by increasing laminating temperature, air permeability was decreased. Furthermore, it only was observed that the adhesive force between layers in multilayer was increased with temperature rise. These results indicate that temperature is an effective parameter for laminating of nanofiber web to make a new type of antibacterial filter media.

Acknowledgement: The authors wish to thank the Iran National Science Foundation (INSF) for their financial support under grant No. 90003694.

References

1. J. S. KIM, D. H. RENEKER, Poly. Eng. Sci., **39**, 849 (1999).
2 S.A. THERON, E. ZUSSMAN ,A.L. Yarin, Polymer, **45**(6), 2017(2004).
3. S. H. TAN, R. INAI, M. KOTAKI, S. Ramakrishna, Polymer, **46**, 6128 (2005).
4. A. K. Haghi and M. Akbari, Phys. Stat. Sol. A, **204**, 1830 (2007).
5. S. W. Fang, C. F. Li, D. Y. C. Shih, J. Food Prot., **56**, 136 (1994).
6. N.M. ANGELOVA, I. RASHKOV, V. MAXIMOVA, S. BOGDANOVA, A. DOMARD, Journal of Bioactive and Compatible Polymers, **10**(4)**,** 285 (1995).
7. M. IGNATOVA, N. MANOLOVA, N. MARKOVA, I. RASHKOV, Macromol. Biosci., **9**, 102 (2009).
8. K. M. KIM, J. H. SON, S.-K. KIM, C. L. WELLER, M. A. HANNA, J. Food Sci., **71**(3), 119 (2006).
9. P. SORLIER, A. DENUZIERE, C. VITON , A. DOMARD, Biomacromolecules, **2**(3), 765 (2001).
10.I.M. HELANDER, E.L. NURMIAHO-LASSILA, R. AHVENAINEN, J. RHOADES, S. ROLLER, International
Journal of Food Microbiology, **71**(2–3), 235 (2001).
11. S.H. LIM, S.M. HUDSON, Journal of Macromolecular Science-Polymer Reviews, C**43**(2), 223 (2003).
12. F. DEVLIEGHERE, A. VERMEULEN, J. DEBEVERE, Food Microbiol., **21,** 703 (2004).
13. I. ARANAZ, M. MENGÍBAR, R. HARRIS, I. PA OS, B. MIRALLES, N. ACOSTA, G. GALED, Á. HERAS, Curr. Chem. Biol., **3**, 203 (2009).
14. A. NEAMNARK, R. RUJIRAVANIT, P. Supaphol, Carbohydr. Polym., **66**, 298 (2006).
15. B. DUAN, C. DONG, X. YUAN, K. YAO, J. Biomater. Sci. Polym. Ed., **15**, 797 (2004).
16. Y. T. JIA, J. GONG, X. H. GU, H. Y. KIM, J. DONG, X. Y. SHEN, Carbohydr. Polym., **67**, 403 (2007).
17. H. HOMAYONI, S. A. H. RAVANDI, M. Valizadeh, Carbohydr. Polym., **77**, 656 (2009).
18. X. GENG, O.-H. KWON, J. JANG, Biomaterials, **26**, 5427 (2005).
19. S. D. VRIEZE, P. WESTBROEK, T.V. CAMP, L.V. LANGENHOVE, J. Mater. Sci., **42**, 8029 (2007).
20. K. OHKAWA, D. CHA, H. KIM, A. NISHIDA, H. YAMAMOTO, Macromol. Rapid Commun. , **25**, 1600 (2004).
21. S. IIJIMA, Nature, 354, **56** (1991).
22.. A. M. K. ESAWI, M.M. Farag, Mater. Design, **28**, 2394 (2007).
23. A. PEDICINI AND R. J. FARRIS, Polymer, **44**, 6857 (2003).
24. K. H. LEE, B. S. LEE, C. H. KIM, H. Y. KIM, K. W. KIM, C. W. NAH, Macromol. Res. **13**(5), 441(2005).
25. H. SCHREUDER-GIBSON, P. GIBSON, K. SENECAL, M. SENNETT, J. WALKER, W. YEOMANS, D. ZIEGLER, P.P. TSAI, J. Adv.Mater., **34**, 44 (2002).
26. L. LIU, Z. M. HUANG, C. L. HE, X. J. HAN, Mater. Sci. Eng. A **435-436**, 309 (2006).
27. M. KANAFCHIAN, M. VALIZADEH, A. K. HAGHI, Korean J. Chem. Eng., **28**(2), 445 (2011).
28. M. KANAFCHIAN, M. VALIZADEH, A. K. HAGHI, Korean J. Chem. Eng., **28**(3), 763 (2011).
29. W. FUNG, Coated and laminated textiles, 1st ed, Woodhead Publishing, 2002, p. 63.
30. S. LEE, D. KIMURA, K.H. LEE, J. C. PARK, I.S. KIM, Textile Res. J., **80**, 99 (2010).
31. Z. M. MAHDIEH, V. MOTTAGHITALAB, N. PIRI, A. K. HAGHI, Korean J. Chem. Eng., **29**(1), 111 (2012).
32. K.SAKURAI, T.MAEGAWA, T. TAKAHASHI, Polymer, **41,** 7051 (2000).
33. M.ZENG, Z.FANG, C. XU, J. Membr. Sci., **230**, 175 (2004)

Manuscript received: 17.04.2012